

# LES AND EXPERIMENTAL STUDY OF SELF-IGNITION OF SUPERSONIC HYDROGEN AND METHANE-HYDROGEN JETS IN A VITIATED CONFINED SUPERSONIC AIR STREAM

**Erwin GEORGE**

Gaz de France, Research and Development Division,  
361, avenue du Président Wilson - BP. 33  
93211 Saint-Denis La Plaine Cedex, France  
erwin.george@gazdefrance.com

**Vladimir Sabel'nikov, Philippe Magre**

ONERA, Fundamental and Applied Energetics Department,  
Fort de Palaiseau, Chemin de la Hunière  
91761 Palaiseau Cedex, France  
vladimir.sabelnikov@onera.fr , philippe.magre@onera.fr

## ABSTRACT

The aim of this work is the comparative study of the self-ignition of hydrogen and methane-hydrogen mixture supersonic jets in vitiated confined supersonic airflow. Self-ignition in this configuration was studied by one of the authors in the ONERA's LAERTE test facility designed for the fundamental study of supersonic combustion. The data, that were collected in the combustor are used to validate LES simulations. Planar Laser Induced Fluorescence (PLIF) measurements of the hydroxyl radical were performed to detect the flame structure. The images showed that self-ignition appears in small-scale pockets (spots), comprising fuel and hot air, and randomly distributed in the air-fuel mixing layer. It is concluded that the self-ignition delay lengths cannot be predicted from delay induction times for homogeneous mixtures, because of large effect of turbulent mixing on the preignition chemistry in the pockets. LES subgrid mixing model is developed to reproduce the observed experimental data.

## INTRODUCTION

Supersonic combustion is a problem of a great fundamental and practical interest, since supersonic ramjets (scramjets) are promising for future airbreathing systems. The further development of scramjets can be significantly aided by the use of CFD. The phenomenon of self-ignition in turbulent supersonic flows is one of the most important for better understanding and ability to predict the complex thermo-fluid dynamics of supersonic reacting flows. Conventional approach towards to self-ignition in inhomogeneous turbulent flows is based on the use of "mixing times" and on the following autoignition delays times in the homogeneous configurations. Recent studies by Markides and Mastorakos (1991) showed that conventional approach is not adequate for self-ignition phenomenon in inhomogeneous subsonic flows. The situation is even more harder for the self-ignition in supersonic

flows. Shocks waves, rarefaction waves and viscous heating have great impact on the self-ignition process. The experimental studies of self-ignition in turbulent supersonic flows are sparse. Self-ignition of sonic hydrogen jet in coflow supersonic ( $M = 2$ ) vitiated air was investigated by Cheng et al. (1994). Self-ignition of supersonic ( $M = 2$ ) hydrogen, ethylene-hydrogen, and methane-hydrogen jets in vitiated confined supersonic stream was examined in ONERA's LAERTE test facility by P. Magre (Magre and Bouchardy, 2000, Magre and Sabel'nikov, 2002). Methane-hydrogen self-ignition data are reproduced in the Davidenko's thesis (2005). PLIF measurements of  $OH$  radical were done to detect the flame structure. The instantaneous images showed that self-ignition proceeds in small-scale pockets, comprising the mixture of fuel, and hot air, and randomly distributed in the supersonic fuel-air mixing layer. The data collected in the combustor were intended to be used for validation of CFD models, and LES in particular. At the present time numerical studies of LAERTE data were based on a RANS approach (Davidenko, 2005) without taking into account turbulence-chemistry interaction. LES was applied by Dauptain (2006) for simulation of hydrogen free jet self-ignition data (Cheng et al., 1994).

This paper deals mainly with LES application to simulate LAERTE self-ignition data for hydrogen and methane-hydrogen mixture. Short description of the LAERTE combustor is also given.

## LAERTE EXPERIMENTAL SET-UP

The LAERTE test facility consists of the following major components: the flame preheater, supersonic nozzle, the optically accessible combustor, hydrogen, hydrocarbons, and air flow loops, combustion products exhaust system. The combustor configuration is shown schematically in Fig. 1. The combustor consisted of two segments: 1) a  $45 \times 45 \text{ mm}^2$  constant cross-section area duct of 370 mm long; 2) a slightly divergent duct

Table 1: Experimental conditions

	Air	H <sub>2</sub>	73%CH <sub>4</sub> - 27%H <sub>2</sub>
$M$	2	2	2
$P_s$ (MPa)	0.08	0.08	0.08
$T_t$ (K)	1850	300	300
$T$ (K)	1200	160	160
$\dot{m}$ (g/s)	650	6,2	7.4 + 2.8
$U$ (m/s)	1336	1970	1600

of 500 mm long with 1.15 degree expansion along the top and bottom walls (i.e. divergence angle of 2.3 degree). The combustor was connected directly to a supersonic Mach 2 nozzle. The air is preheated first up to 850K in a primary heat exchanger, and then up to 1850K in the flame hydrogen-air heater with oxygen replenishment to obtain a test gas with the same oxygen mole fraction as atmospheric air (0.2095). Water vapors were around 16 percent molar fractions. Air mass rate was typically 650 g/s. Static pressure at the combustor entrance was 0.08 MPa. A water-cooled axisymmetrical supersonic fuel injector of internal diameter  $d = 6$  mm (external diameter is 10 mm) was installed along the axis of the nozzle. Injector exit section was at  $x_{inj} = 33$  cm downstream of combustor entrance. Supersonic (Mach 2) fuel jets were adapted to the static pressure at the combustor entrance. Optical access was obtained via silica windows mounted in the side plates of the test section at three places:  $6 < (x - x_{inj})/d < 15$ ,  $26 < (x - x_{inj})/d < 34$ , and  $37 < (x - x_{inj})/d < 43$ . More details on the combustor and test facility can be found elsewhere in works by Magre (Magre and Bouchardy, 2000, Magre and Sabel'nikov, 2002). Operating conditions used here for LES validation are summarized in Table 1.  $M$ ,  $P_s$ ,  $T_t$ ,  $T$ ,  $\dot{m}$ ,  $U$  stands for the Mach number, static pressure, total temperature, static temperature, mass flow rate, and velocity, respectively.

## EXPERIMENTAL RESULTS

### Pressure Distributions

Because of hostile environment of the high-temperature reacting supersonic flow, the only parameter measured systematically is the mean wall pressure distribution along the combustor. To determine the location where the ignition starts, the wall pressure distributions for both a non-reacting case (using nitrogen instead of fuel) and a reacting case are compared. The self-ignition delay length is determined as the distance between the injector exit section and the location where reacting pressure distribution starts to grow in comparison with non-reacting one.

Experimental wall pressure distributions for pure hydrogen and 73 percent CH<sub>4</sub> - 27 percent H<sub>2</sub> (mass fractions) mixture jets, respectively, are given in Fig. 2. Wall pressure is normalized by the plenum  $P_t$  pressure (stagnation pressure in the heater). The estimated self-ignition lengths are, 15 cm and 33 cm, respectively.

### PLIF Images

Instantaneous PLIF images have revealed that the self-ignition proceeds in two stages. As a typical example, instantaneous PLIF images for the pure hydrogen jet are given in Fig. 3. Close to the injector ( $6 < (x - x_{inj})/d < 15$ ), a large number of small-scale (less than 1 mm) and short lifetime pockets in intermittent combustion are observed, Fig. 3 (a). Downstream this location, for  $26 < (x - x_{inj})/d < 34$ , PLIF images show larger and more long lifetime pockets, of scale 5 mm, of mixed hot air, fuel, and of combustion products generated upstream, Fig. 3 (b).

The most important conclusions for the PLIF images are that:

- self-ignition has a spotty character and appears in the form of random pockets
- self-ignition involves the intricate interplay between the mixing and the chemistry
- each pocket has its unique history, as a consequence mixing and the self-ignition chemistry cannot be decoupled
- flamelet models cannot be used for LES modeling self-ignition in turbulent supersonic stream

## LES MODELING

### Governing Equations

For the sake of brevity, LES equations for the compressible Navier-Stokes equations are not given here (see, e.g., Sankaran et al., 2004). Smagorinski subgrid-scale model was used for the eddy viscosity. Smagorinski model constant is taken  $C_S = 0.18$ , turbulent Prandtl number is  $Pr_t = 0.9$ , and turbulent Schmidt number is  $Sc_t = 0.7$ .

### Subgrid Scalar Mixing Model

The filtered reaction rate term  $\overline{\dot{\omega}_k}$  requires closure. PLIF images revealed that self-ignition in turbulent supersonic flow appears in random pockets. Here Partially Stirred Reactor (PaSR) model is used to describe turbulence-chemistry interaction at the subgrid-scale level. Among existing PaSR models, the Vulis model (VM), Vulis (1961), was chosen as most simple and well adapted for costly LES computations. Original version was formulated for homogeneous stationary reactor. Stationary Vulis model was extended (EVM) in this paper for the calculation of  $\overline{\dot{\omega}_k}$  (George, 2007). The filtered reaction rate is calculated from:

$$\overline{\dot{\omega}_k} = \dot{\omega}_k(Y_{v,k}, T_v) \quad , \quad (1)$$

where  $Y_{v,k}$  is linked with filtered mass fraction  $\widetilde{Y}_k$ :

$$Y_{v,k} = \widetilde{Y}_k + \tau_m^{sgs} \frac{\dot{\omega}_k(Y_{v,k}, T_v)}{\bar{\rho}} \quad (2)$$

The subgrid-scale mixing time  $\tau_m^{sgs}$  is determined by the resolved turbulent frequency  $\omega$  as:

$$\tau_m^{sgs} = \frac{1}{\omega} \quad \text{with} \quad \omega = \sqrt{2C_S \tilde{S}_{ij} \tilde{S}_{ji}} \quad , \quad (3)$$

$$\tilde{S}_{ij} = \frac{1}{2} \left( \frac{\partial \tilde{u}_i}{\partial x_j} + \frac{\partial \tilde{u}_j}{\partial x_i} \right) \quad . \quad (4)$$

### Computational Details

Simulations were performed with the CFD code CEDRE developed at ONERA. The governing equations are solved using a finite volume scheme that is nominally second order explicit Runge-Kutta integration scheme (second order in time and space). Numerical scheme used in CEDRE is a shock capturing scheme that is well adapted to supersonic flows (Garnier et al., 1999 and Martin, 2000). For this scheme, in explicit formulation, stability, and accuracy are obtained at  $CFL \approx 0.25$ .

Chemistry was modeled by Eklund's mechanism (Eklund et al., 1991) with 9 species and 7 reactions, for the combustion of pure hydrogen in air, and by detailed chemical mechanism from Davidenko (2005) with 21 species and 79 reactions, for methane-hydrogen case. Chemistry is treated implicitly in CEDRE.

The computational domain comprises the space between the injector exit section and the combustor exit located at 837 mm downstream of injector exit. For 2D axisymmetric and 3D calculations 150.000 ( $200 \times 750$ ) and 1.550.000 ( $200 \times 97 \times 80$ ) cells meshes were used. The grids were generated by GMSH for the 2D case and with PROSTAR (StarCD meshing software) for the 3D configuration. The grids points were clustered near the combustor walls and in the supersonic mixing layer formed by the fuel jets and air coflow. The equivalent axisymmetric combustor with the cross-area section of real combustor was used for 2D axisymmetric LES, to keep the same air/fuel mass flow rate.

In order to reduce computational and memory cost, for the 2D case the computational domain has been splitted in two sub-domains (MPI library is used for the communication between the two processors) and calculations were performed with ONERA's vectorial computer NEC SX-5. Concerning the 3D case, the domain was splitted in four different domains (each dedicated to a processor and MPI library is used for the communication between the 4 processors). Computations have been performed with ONERA's vectorial computer NEC SX-8. The analyses showed that the grid was relatively coarse. This fact leads to the numerical over-diffusion as against the Smagorinsky subgrid-scale model for non-reactive case (resulting implicit LES). For reactive case, the Smagorinsky eddy diffusivity prevailed. This result can be explained by larger field gradients in the reactive flows.

All boundary conditions are specified to closely match the experiments. Supersonic inflow and outflow conditions are imposed. The logarithmic law of the wall, and Reynolds analogy for heat transfer coefficient are applied in turbulent boundary layers of the combustor. The turbulence intensity at the inflow section is taken equal to 5 percent for of air and fuel streams. Time integration was carried out with a  $CFL \approx 0.2$ . This small value of CFL number is mainly dictated

by gasdynamic structure of supersonic flow, as was explained above. LES calculations simulate the physical time duration 10 ms for hydrogen jet in 2D or 3D simulations and 7 ms for methane-hydrogen mixture in 2D jet simulations (residence time in the combustor is about 1 ms). A grid independent study was performed as part of the validation procedure. Two different grid resolutions were used for the 2D and 3D cases, and results agree well with each other.

## RESULTS AND DISCUSSION

### 2D Simulations

Because of the computation time limitations, most of the calculations were performed with 2D approach (see also George et al., 2005, 2006). Control 3D LES calculations showed quite small difference from 2D LES. We will present this comparison further.

**Non-Reactive Case.** Estimated expansion rate of supersonic  $N_2$ -air mixing layer is about 5 percent and is in good agreement with experiment (Magre and Bouchardy, 2000, Magre and Sabel'nikov, 2002). Fig. 4 shows the comparison of mean wall pressure (normalized by plenum pressure) distributions in combustor (30 realizations and also time averaging were used to calculate mean values) and experimental data (with  $N_2$  injection). By comparing two LES results (inert  $H_2$  and  $N_2$ ), we find the small difference. The agreement with experiment can be considered sufficiently good. Fig. 5 shows the profile of mean axial velocity at  $(x - x_{inj}) = 33$  mm along with PIV measurements. The agreement is satisfactory.

**Reactive Case. Pure Hydrogen Jet.** Fig. 6 shows an instantaneous snapshot of  $OH$  field for  $10 < (x - x_{inj})/d < 15$ . There is qualitative correspondence between Figs. 3 and 6: both show the spotty character of combustion in instantaneous fuel-air mixing layer. Fig. 7 shows the normalized mean wall pressure distribution along the combustor with the experimental data. The agreement is quite good both with and without subgrid-scale mixing model. The estimated self-ignition delay length is about 15 cm. RANS calculations by Davidenko (2005) show practically the absence of delay length. Fig. 8 presents the mixing  $\eta_{mix}$  and combustion  $\eta_c$  efficiencies along the combustor. The mixing efficiency was calculated from the following equations:

$$\eta_m(x) = \frac{\dot{m}_{mix}}{\dot{m}_Z} \quad , \quad (5)$$

$$\dot{m}_{mix} = \int \int \frac{\tilde{Z}}{\max(\phi, 1)} \tilde{\rho} \tilde{u} dS_x \quad , \quad \dot{m}_Z = \int \int \tilde{Z} \tilde{\rho} \tilde{u} dS_x \quad (6)$$

$$\phi = \frac{\tilde{Z}}{1 - \tilde{Z}} \frac{1 - Z_{st}}{Z_{st}} \quad , \quad Z_{st} = \frac{1}{1 + r} \quad , \quad \tilde{Z} = \frac{Y_{N_2}^{air} - \tilde{Y}_{N_2}}{Y_{N_2}^{air}} \quad . \quad (7)$$

where  $\tilde{Z}$  is the Favre-filtered mixture fraction mea-

suring the local air/fuel ratio,  $r$  is the stoichiometric air-fuel ratio,  $\tilde{Y}_{N_2}$  is the Favre-filtered nitrogen mass fraction,  $Y_{N_2}^{air}$  is the mass fraction of nitrogen in vitiated air. The ratio  $\tilde{Z}/max(\phi, 1)$  represents the fraction of the fuel that is able to burn.  $S_x$  is the cross section area at section  $x$ .

Combustion efficiency was calculated from equations:

$$\eta_c(x) = 1 - \frac{\dot{m}_f}{\dot{m}_{mix}}, \quad \dot{m}_f = \int \int \tilde{Y}_{fuel} \tilde{\rho} u dS_x, \quad (8)$$

where  $\tilde{Y}_{fuel}$  is the Favre-filtered fuel mass fraction. From Fig. 8 (a) we conclude that overall mixing efficiency  $\eta_{mix}$  at the end of self-ignition delay length is relatively small,  $\eta_{mix} \approx 0.05 - 0.07$ . Nevertheless, this level of preliminary mixing is sufficient for thermal runaway of chemically active fuel, as  $H_2$ . The maximal total temperature axial distribution is shown in Fig. 8 (b). To see the supersonic flame structure, instantaneous snapshots of static pressure,  $OH$  radical, species  $H_2$ ,  $H_2O$  and static pressure are presented in Fig. 9.

As a consequence of small mixing efficiency, the self-ignition of pure hydrogen is characterized by the moderate rate of wall pressure rise due to a slowly increasing heat release. Instantaneous snapshots of Mach number field (not shown here) demonstrate that the flow remains supersonic over the whole combustor length.

**Reactive Case. Methane-Hydrogen Mixture.** Addition of methane to hydrogen results in chemically less active fuels. Fig. 10 shows the normalized mean wall pressure distributions along with experimental data. Experimental self-ignition delay can be estimated as about 33 cm. LES with subgrid-scale mixing model reproduces this delay. LES without subgrid-scale mixing model results in the premature self-ignition: the calculated mean wall pressure departs from non reacting case at  $x - x_{inj} = 25$  cm. The LES without subgrid-scale mixing model also overestimates the pressure rise due to heat release in the region  $25 \text{ cm} < (x - x_{inj}) < 50$  cm. Fig. 11 shows the mixing and combustion efficiencies. Overall mixing efficiency before self-ignition is around of 0.3, and larger in comparison with pure hydrogen jet (Fig. 8). It is explained by lesser chemical activity of methane-hydrogen mixture with respect to pure hydrogen. The flow remains supersonic at the whole combustor length, as it follows from the instantaneous snapshots of Mach number field (not shown here). Finally, we note that self-ignition length with RANS calculations (Davidenko, 2005) is around 10 cm.

### 3D Simulations

3D hydrogen LES calculations were performed on the 1.500.000 nodes mesh. Calculations correspond to 8 ms and 6 ms of physical time for non-reactive and reactive cases, respectively. Fig. 12 shows the normalized mean wall pressure distributions, obtained by the comparison of 3D and 2D LES calculations, for non-reactive (Fig. 12 (a)) and reactive cases (Fig. 12 (b)) along with experiments. Pressure distributions with 3D calculations are slightly above of ones

with 2D. This result is explained by somewhat larger subgrid-scale mixing with 3D effects taken into account. Nevertheless, 2D and 3D LES results are in reasonable agreement.

### CONCLUSION

In the present work the comparative study of the self-ignition of pure hydrogen and methane-hydrogen mixture supersonic jets in a supersonic ONERA's LAERTE combustor has been carried out. The study comprises both LES and experimental investigations.  $OH$ -PLIF measurements were done to detect the flame structure. The PLIF images and subsequent analyses showed that self-ignition has a spotty character and proceeds in sufficiently small-scale pockets, comprising the mixture of fuel, and hot air and randomly distributed in the fuel-air supersonic mixing layer. LES have been carried out to simulate LAERTE combustor self-ignition data. Smagorinsky subgrid-scale eddy diffusion closure is coupled with the extended Vulis PaSR mixing model (EVM) to treat turbulence - combustion interaction. Detailed chemical kinetics mechanisms are used for hydrogen and methane-hydrogen mixtures. LES computations predict reasonably well the experimental data.

### REFERENCES

- Cheng, T.S. and Wehrmeyer, J.A. and Pitz, R.W. and Jarrett, O. and Northam, G.B., 1994, "Raman Measurement of Mixing and finite-rate chemistry in a supersonic hydrogen-air diffusion flame", *Combustion and Flame*, Vol. 99, pp. 157-173.
- Dauptain, A., 2006, "Allumage des moteurs fusées cryotechniques", Ph. D. Thesis CERFACS/INP Toulouse.
- Davidenko, D., 2005, "Contribution au développement des outils de simulation numérique de la combustion supersonique", Ph. D. Thesis LCSR/Université d'Orléans.
- Eklund, D.R. and Drummond, J.P. and Hassan, H.A., 1991, "Calculation of supersonic turbulent reacting coaxial jets", *AIAA Journal*, Vol. 28(9), pp.1633-1641.
- Garnier, E. and Mossi, E. and Sagaut, P. and Comte, P. and Deville, M., 1999, "On the use of shock-capturing schemes for large eddy simulations", *Journal of Computational Physics*, Vol. 153, pp. 273-311.
- George, E., 2007, "Modélisation et Simulations numériques de l'auto-allumage de élanges hydrocarbures-hydrogène dans un écoulement supersonique coaxial confiné d'air chaud", Ph. D. Thesis ONERA/INSA de Rouen.
- George, E. and Magre, P. and Sabel'nikov, V., 2003, "Self-ignition of Hydrogen-Hydrocarbons Mixtures in a Hot Supersonic Confined Coflow of Air", 13th AIAA/CIRA International Space Planes and Hypersonics Systems and Technologies, 9-12 May, Capua, Italy, AIAA Paper 2005-3393.
- George, E. and Magre, P. and Sabel'nikov, V., 2006, "Numerical Simulations of Self-Ignition of Hydrogen-Hydrocarbons Mixtures in a Hot Supersonic Airflow", 42nd AIAA/ASME/SAE/ASEE Joint

Propulsion Conference and Exhibit, 9-12 July, Sacramento, California, USA, AIAA Paper 2006-4611.

Magre, P. and Bouchardy, P., 2000, "Nitrogen and Hydrogen CARS Thermometry in a Supersonic reactive Mixing Layer", Proceedings of the Combustion Institute, Vol. 28, pp. 697-703.

Magre, P. and Sabel'nikov, V., 2002, "Self-Ignition of Hydrogen-Ethylene Mixtures in a Hot Supersonic Air Flow", 11th AIAA/AAAF International Space Planes and Hypersonics Systems and Technologies, 29 September - 4 October, Orléans, France, AIAA Paper 2002-5205.

Markides, C.N. and Mastorakos, E., 2005, "An experimental study of hydrogen autoignition in a turbulent coflow of heated air", Proceedings of the Combustion Institute, Vol. 30, pp. 883-891.

Martin, M.P., 2000, "Shock-capturing in LES of high-speed flows", Center of Turbulence Research, Annual Research Briefs.

Sankaran, V. and Genin, F. and Menon, S., 2004, "A sub-grid mixing model for large eddy simulation of supersonic combustion", AIAA Paper 2004-0801.

Vulis, V., 1961, "Thermal Regime of Combustion", McGraw-Hill, New-York, (Russian edition 1954), Chap. 3.

**FIGURES**

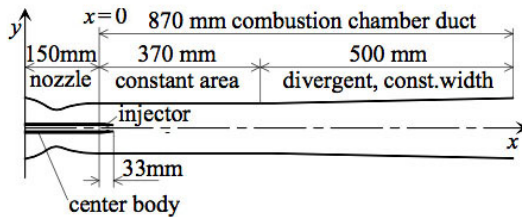


Figure 1: Scheme of the LAERTE experimental test facility

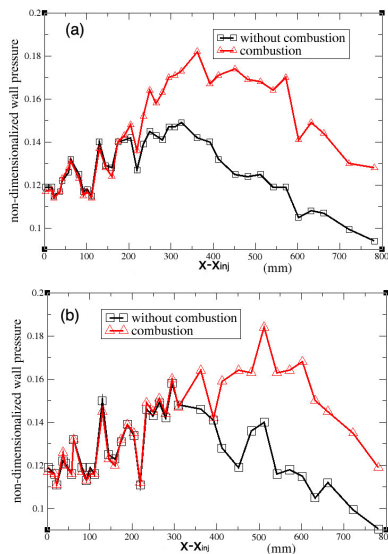


Figure 2: Normalized mean wall pressure distribution along the combustor: (a) pure hydrogen, (b) 73 percent methane - 27 percent hydrogen mixture (in mass fractions)

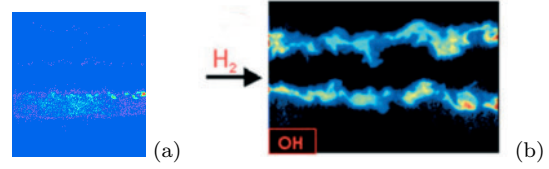


Figure 3: Instantaneous PLIF images of OH radicals: (a) close to the injector ( $6 < (x - x_{inj})/d < 15$ ), (b) far from the injector ( $26 < (x - x_{inj})/d < 34$ )

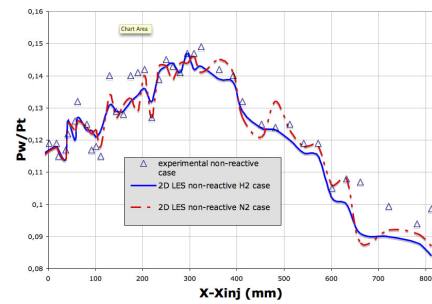


Figure 4: Normalized mean wall pressure distributions along the combustor; non-reactive case

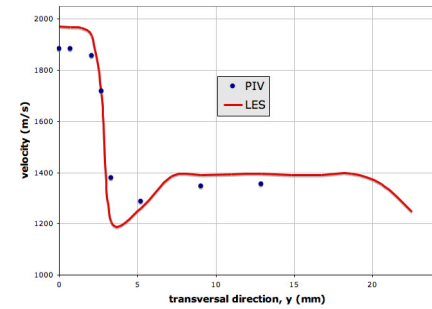


Figure 5: Comparison PIV/LES for axial velocity

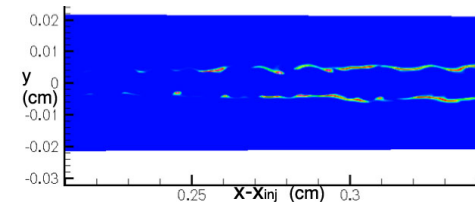


Figure 6: Instantaneous snapshot of OH radical,  $10 < (x - x_{inj})/d < 15$

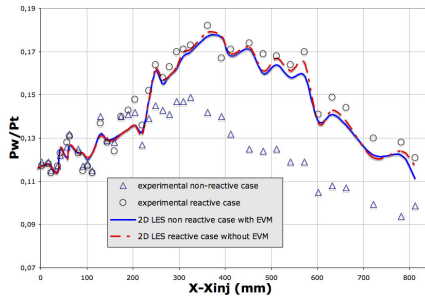


Figure 7: Normalized mean wall pressure distributions along the combustor for hydrogen reacting case

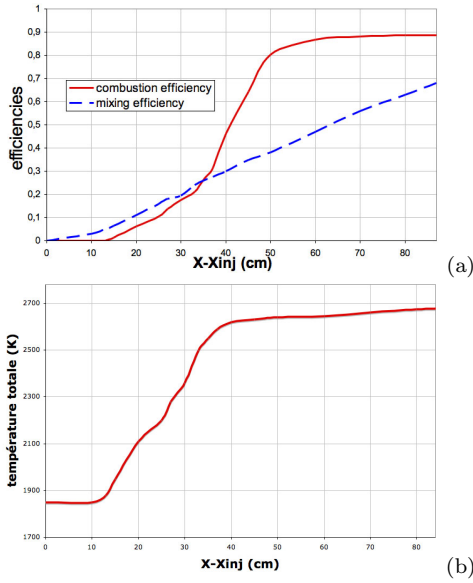


Figure 8: Axial distributions for pure hydrogen: (a) mixing and combustion efficiencies, (b) maximal total temperature

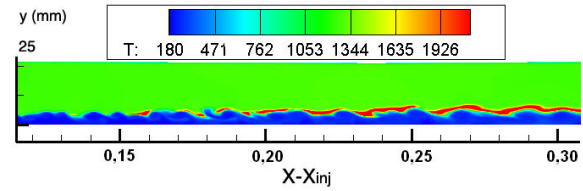
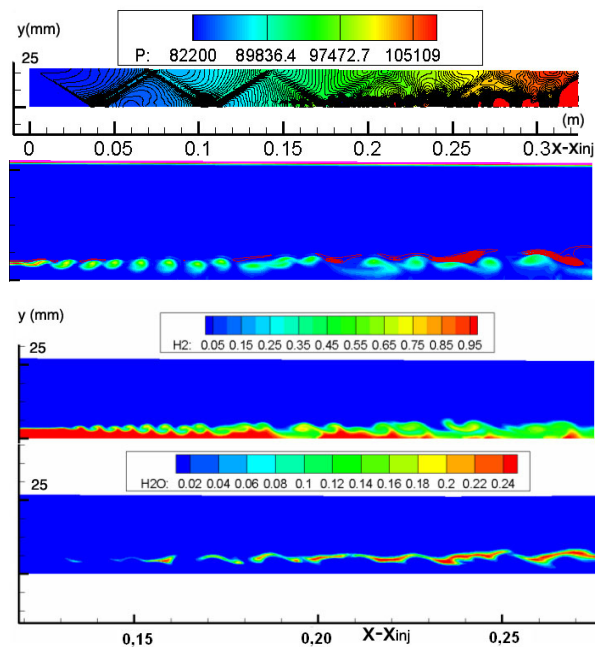


Figure 9: Instantaneous snapshots for pure hydrogen case; from top to bottom: static pressure,  $OH$  radical, species  $H_2$ ,  $H_2O$ , and static temperature (K)

Figure 10: Normalized mean wall pressure distributions along the combustor obtained with 2D LES simulations of methane-hydrogen injection

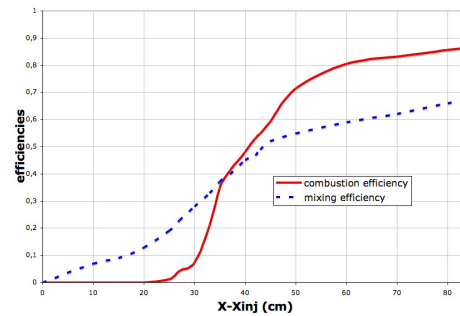


Figure 11: Mixing and combustion efficiencies axial distributions for methane-hydrogen mixture

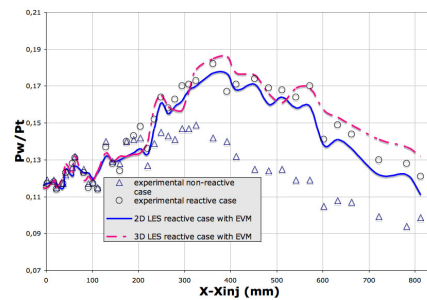


Figure 12: Comparison of normalized mean wall pressure distributions along the combustor obtained with 2D and 3D LES simulations of pure hydrogen injection